Experimental and ab initio DFT calculated Raman spectrum of Sudan I, a red dye

ARTICLE *in* JOURNAL OF RAMAN SPECTROSCOPY · JUNE 2011

Impact Factor: 2.67 · DOI: 10.1002/jrs.2876

4 AUTHORS, INCLUDING:

Andreas J. Kunov-Kruse
Technical University of Denmark
11 PUBLICATIONS **85** CITATIONS
SEE PROFILE

Steffen Buus Kristensen
Haldor Topsøe
7 PUBLICATIONS **79** CITATIONS
SEE PROFILE

Rolf W. Berg
Technical University of Denmark
179 PUBLICATIONS **2,235** CITATIONS
SEE PROFILE

Research Article

Journal of RAMAN SPECTROSCOPY

Received: 15 October 2010 Accepted: 23 November 2010 Published online in Wiley Online Library:

(wileyonlinelibrary.com) DOI 10.1002/jrs.2876

Experimental and *ab initio* DFT calculated Raman spectrum of Sudan I, a red dye

Andreas J. Kunov-Kruse,[a] Steffen B. Kristensen,[a] Chuan Liu[b] and Rolf W. Berg[b]*

The red dye Sudan I was investigated by Raman spectroscopy using different excitation wavelengths (1064, 532 and 244 nm). A calculation of the Raman spectrum based on quantum mechanical *ab initio* density functional theory (DFT) was made using the RB3LYP method with the 3-21G and 6-311+G(d,p) basis sets. The vibrations in the region 1600–1000 cm^{-1} were found to comprise various mixed modes including in-plane stretching and bending of various C–C, N–N, C–N and C–O bonds and angles in the molecule. Below ~900 cm^{-1}, the out-of-plane bending modes were dominant. The central hydrazo chromophore of the Sudan I molecule was involved in the majority of the vibrations through N=N and C–N stretching and various bending modes. Low-intensity bands in the lower wavenumber range (at about 721, 616, 463 and 218 cm^{-1}) were selectively enhanced by the resonance Raman effect when using the 532 nm excitation line. Comparison was made with other azo dyes in the literature on natural, abundant plant pigments. The results show that there is a possibility in foodstuff analysis to distinguish Sudan I from other dyes by using Raman spectroscopy with more than one laser wavelength for resonance enhancement of the different bands

Keywords: azo dye; DFT calculation; Sudan I; resonance enhancement

Introduction

In recent years, public attention has been drawn to a group of red and orange azo dyes comprising Sudan I, II, III and IV. Several European control authorities have discovered the presence of these cheap dyes in a series of imported food items.[1] Especially, Sudan I (Fig. 1) is considered to be toxic, and it has been proven by *in vitro*[2,3] and *in vivo* studies that it is carcinogenic to rats, which are known to have a metabolic system very similar to that of humans. Therefore, Sudan I could be carcinogenic to humans as well.[2–4] A series of detection methods have been developed, most of them based on liquid chromatography.[1,5–7] The recently applied methods for Sudan I give detection limits on the order of around 0.5 ppm.[2] No known threshold limit seems to exist with respect to long-term health risks, and therefore there is a need for further development of the detection methods.

Raman spectroscopy can offer a novel and fast method for *in situ* and on-location detection of Sudan dyes during food control. The detection of Sudan I by surface-enhanced Raman scattering (SERS) spectroscopy and surface-enhanced resonance Raman scattering (SERRS) spectroscopy can offer very accurate analysis methods with detection limits below 0.20 ppm.[8] Although the methods have been demonstrated, the extent of scientific literature on the Raman spectra of Sudan dyes is very limited, with very few articles having been published so far. Thus until recently, only SERS spectra of Sudan II and IV were reported,[9,10] with only two articles dealing with spectra of Sudan I: the first one[11] by using a range of excitation lines, with respect to resonance Raman (RR), SERS and SERRS, as well as a calculated spectrum by the use of low-level PM3 semiempirical methods; and the second one[12] using a portable spectrometer with SERS and multivariate chemometrics to obtain quantitative analysis down to 10^{-4} mol l^{-1}.

A deeper understanding of the chemistry and structure of these planar molecules is needed to develop a Raman-based precise method that will be able to distinguish the Sudan molecules from other azo dyes. The current problem of distinguishing Sudan I from naturally abundant carotenoids – especially capsanthin – is difficult because of the almost identical absorption maxima,[2,13] and this will be treated in the present article.

In the following, first, new and better *ab initio* DFT calculations are presented. Then the experimental Raman spectra of Sudan I with different excitation wavelengths are given, followed by an attempt to correlate the experimental vibrational peaks in the Raman spectrum to the results of the DFT calculations in order to understand the nature of the vibrations in the Sudan I molecule. Finally, we will make some general conclusions about the characteristic vibrations in the Sudan group of molecules, based on the measured spectra, in comparison with the calculations and spectra from the literature.

Structure of Sudan I

The structure of azo dyes has been intensely discussed in the chemical literature. The azo dyes formally contain the azo group –N=N–, but are in most cases partly or completely transformed into the tautomeric hydrazo form (Scheme 1). Initially our geometry optimizations were done on both forms. However,

* *Correspondence to: Rolf W. Berg, Department of Chemistry, Technical University of Denmark, Kemitorvet, Building 207, DK-2800 Kgs. Lyngby, Denmark. E-mail: rwb@kemi.dtu.dk*

a *Center for Catalytic and Sustainable Chemistry; Department of Chemistry, Technical University of Denmark, Kemitorvet, DK-2800 Kgs. Lyngby, Denmark*

b *Department of Chemistry, Technical University of Denmark, Kemitorvet, Building 207, DK-2800 Kgs. Lyngby, Denmark*

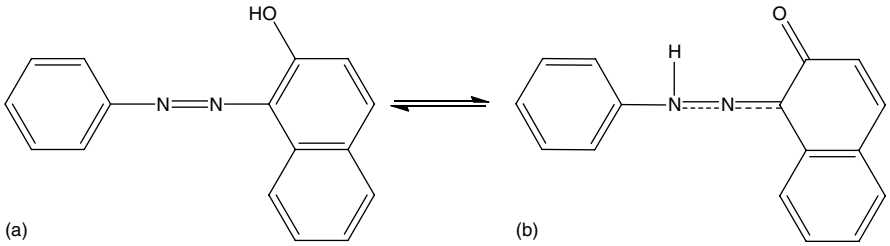

Scheme 1. The tautomeric inversion of Sudan I: (a) the azo form and (b) the hydrazo form. The equilibrium is shifted far to the right.

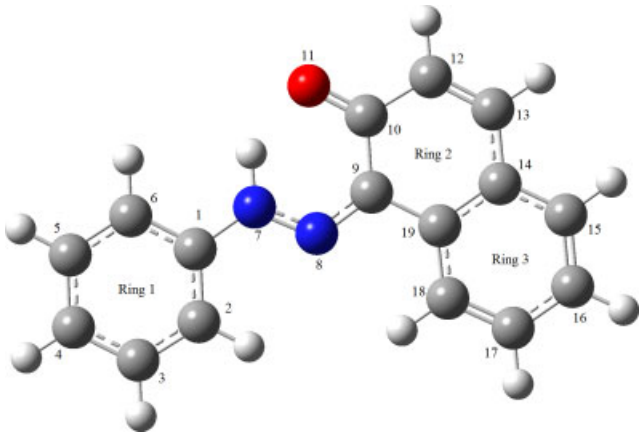

Figure 1. The optimized structure of Sudan I. C: carbon, N: nitrogen and O: oxygen. The numbers 1–19 refer to the numbering of C, N and O atoms in the molecule. The same numbering also refers to the H atoms adjacent to the C, N and O atoms.

the azo forms gave poor resemblance to the experimental spectrum irrespective of whether the H atom on O was pointing away from or toward the nearest N (giving minimum energies of −801.8223 or −801.8449 a.u. and dipole moments of 1.7653 or 1.0586 debye, respectively). In contrast to this, the calculated spectrum for the hydrazo form showed good resemblance to the experimental spectrum (giving a lower minimum energy of −801.8470 a.u. and a dipole moment of 1.6966 debye). These observations are supported by results in the literature,[11] in which Sudan I was found to be exclusively in the hydrazo form. Therefore, we only report our hydrazo results. The recently published work[12] on SERS analysis of Sudan I, unfortunately, does not mention the hydrazo form and the results were discussed as if Sudan I was in the azo form.

Experimental

Sudan I ($C_{16}H_{12}N_2O$, 1-(2-phenyldiazenyl)-2-naphthalenol, CAS Reg. no. 842-07-9) in pure powder form, obtained from Aldrich, was used without further purification in all experiments. Extra virgin olive oil (low acidic, from Italy) and dichloromethane (CH_2Cl_2, CAS Reg. no. 75-09-2) in pure state (Merck, Pro Analysi grade) were used as solvents to dissolve Sudan I. The solutions (nearly saturated) were made to avoid melting and decomposition of the red dye sample during illumination due to its strong absorption of green and blue light.[1] A DILOR-XY (Horiba-JY) Raman spectrometer was used in the visible range by applying a few milliwatts of radiation at 532 nm (from a Nd : YVO_4 laser equipped with a frequency-doubling device based on crystalline LiB_3O_5). A beam-splitter-coupled optical microscope was used to focus the laser beam onto the sample and to collect the light. The Rayleigh scattered light was filtered off by using a notch filter, and the remaining scattered light was dispersed by a 1800 g mm^{-1} grating and collected on a charge-coupled device (CCD) cooled to 140 K with liquid nitrogen. The broad background due to, e.g. fluorescence was stepwise fitted with second- or third-order polynomials and subtracted from each frame before merging to obtain the spectrum. Calibration was done using the Raman lines of cyclohexane. Both the solvent and the saturated solution were measured as drops on an aluminum foil or (for CH_2Cl_2) inside thin-walled quartz capillaries to avoid decomosition. The UV excitation was obtained with a frequency-doubled Ar^+ LEXEL gas laser working at 488 nm to obtain up to 100 mW of 244 nm radiation. The UV-excited spectra (resolution ~8 cm^{-1}) were recorded with a Renishaw InVia Raman microscopy spectrometer with UV optics, high bandpass filters and an UV-enhanced CCD detector cooled to low temperatures. The measurements were repeated in the infrared range on a Bruker-IFS66 FRA-106 Fourier transform Raman spectrometer by using about 100 mW of Nd : YAG IR laser light at 1064 nm. Two hundred scans were recorded and averaged for each spectrum. Further details on the used Raman spectrometers are described elsewhere.[14–17]

Computations

The optimization of the structure and the calculation of spectra were performed with the Gaussian 03 W software package.[18] The structure of the Sudan I molecule and its vibrations (in both its azo and hydrazo forms) were obtained in three subsequent calculations, in order to determine the global minimum in an efficient way. Initially, each geometry was roughly optimized using the semiempirical PM3 type procedure, followed by the *ab initio* Hartree–Fock/DFT method with third order restricted Becke–Lee–Yang–Parr procedure (RB3LYP), first with the 3-21G basis sets and then using 6-311+G(d,p) basis sets to calculate the structure and vibrational spectra. The scaling factor was chosen to be 0.976 on the basis of results from Ref. [19], where a number of calculated and experimental spectra of C-, H-, N- and O-containing compounds were compared using several basis sets to find the best scaling factor.

Results and Discussion

The obtained Raman data can be seen in Fig. 2, showing the spectra of the pure solvents, olive oil (a) and dichloromethane (c) and (e), of Sudan I dissolved in these solvents (b), (d) and (f), and of the pure Sudan I (g), under different kinds of laser excitation, together with the calculated Raman spectrum. The spectra of

dichloromethane were in accordance with those reported in the literature.[20] A summary of the measured and calculated spectra is shown in Table 1, as well as the approximate assignments of the vibrational modes, derived from the calculations and read off a computer screen by the use of the GaussView G03W program.[18]

The spectrum of the Sudan I dissolved in the solvents olive oil (Fig. 2(b)) or in CH_2Cl_2 (Fig. 2(d) and (f)), showed practically no characteristic bands due to the solvents, even though these solvents have very strong bands (Fig. 2(a),(c) and (g)). The reason must be that Sudan I, as a solute, gives a very strong spectrum. Most probably, this is due to RR enhancement effects, which are different for green (b) and (d) and UV excitation (f). The spectra obtained with green excitation resemble the FT-Raman spectrum of pure solid Sudan I obtained with infrared excitation (Fig. 2(g)). The intensities of the peaks in the spectra (b) and (d) obtained with green light were very similar, except in the region below 900 cm^{-1} where some of the bands of dissolved Sudan I appeared stronger. In the spectrum obtained with the UV light, the bands around 1600 cm^{-1} are very strongly and selectively enhanced, whereas the other bands are not seen. One might suspect that Sudan I could be sensitive to photolysis during UV illumination, but this does not seem to be the case, judging from the spectrum of the solid. The observed spectrum, as shown in Fig. 3(a), appeared stable and had bands resembling those from the infrared experiment (b) and the calculated spectrum (c).

Assignment of Vibrational Modes

The C–H/N–H stretching transitions appear weakly in both experimental and theoretical spectra. Two very weak bands at 3067 and 3039 cm^{-1} and a shoulder at 3059 cm^{-1} are present, corresponding to C–H and N–H stretchings, correlating to modes 87–76 in Table 1.

A very strong band is present at 1596 cm^{-1} (with several weaker shoulders), very close to the predicted position. This band is assigned to mainly aromatic C–C stretching in the phenyl ring, in accordance with other studies of azo dyes,[21,22] but C–H as well as N–H in-plane bendings also contribute significantly to the mode. A band of medium intensity at 1546 cm^{-1} could be described by mode 69 and 70 transitions, both of which comprise H–N=N bending, C=C strethcing and C=O stretching. For both modes, a strong contribution from N–H in-plane bending seems probable. A strong band at 1494 cm^{-1} and a shoulder at 1481 cm^{-1} probably correspond to modes 68 and 67, respectively, composed of mainly C=C stretching and C–H in-plane bendings. C=O and N=C stretchings are also contributing to mode 67, which is observed as a shoulder. A band at 1448 cm^{-1} of weak to medium intensity is accurately predicted by mode 65, comprising mainly in-plane C–H bending and C=C stretching in the naphtalene unit, as well as in-plane bending of the N–H bond. A very strong peak is located at 1388 cm^{-1} with a significant shoulder at 1410 cm^{-1} and a poorly resolved shoulder at around 1370 cm^{-1}. These features could be explained by modes 63 and 64, which are rather complex and share similarities such as strong C–N stretching and C–H and N–H in-plane bendings as well as some C=C strecthing. Significant N=N stretching and some C=O stretching are also contributing to mode 63. The band of medium intensity at 1340 cm^{-1} with a shoulder at 1333 cm^{-1} would correspond to modes 61 and 60, respectively. Mode 61 consists of C=C stretching and in-plane C–H bending in the naphtalene unit and stretching of the C9–N bond. Mode 60 resembles mode 61, but the phenyl unit is more active in the vibration with respect to C=C stretching and C–H bending, and with pronounced stretching of the N=N bond.

The rest of the region down to around 1018 cm^{-1} is very complex, and the spectrum consists of several bands, some of them strong but most of them showing rather low Raman intensity and appearing only as shoulders or weak bands. At least 13 features in this region could be identified, but judging from the asymmetrical shape of several of these bands, it seems that there are even more features hidden underneath some of the more intense bands. The complexity of the experimental spectrum is in accordance with the calculated spectrum of this region, in which 14 different modes are predicted, most of them of extensively mixed origin. The modes 59 and 58, for example, comprise extensively coupled N=N, C=O, C=C stretchings and in-plane C–H and N–H bendings. In the middle part of the region (for modes 57–53) the amount of C–C stretching is gradually descreasing, whereas the amount of C–C–C angle deformations are increasing the lower the wavenumber region. The C–C stretchings still participate and N–C stretchings also contribute to many of the modes. For the lower wavenumber modes in this region, above 1000 cm^{-1}, the C–C stretchings are taking part actively, but now participating in the ring breathings, resulting in asymmetrical deformations of the aromatic rings.

A doublet of medium intensity is found with peaks at 1001 and 984 cm^{-1}, and these bands are predicted very accurately by modes 45 and 43. Both modes include breathing and deformations. Especially, mode 45 could be described by a triangular ring breathing movement. The mode mainly involves three carbon atoms out of the six-membered ring performing a symmetrical breathing-like deformation, resulting in the ring approaching a triangular shape (Fig. 4, mode 45). In this mode, the phenyl ring and ring 3 of the naphtalene unit are both performing triangular breathing, but are out of phase with each other, thereby cancelling out some of the large change of polarizabillity (and intensity) often seen for aromatic breathing modes. Mode 43 comprises conventional breathing of the phenyl ring and triangular breathing of the naphthalene ring 3, as well as C–N=N and N–H in-plane bendings, resulting in a medium intensity band.

The region below 980 cm^{-1} contains serveral weak bands. In general, these are quite accurately predicted in the calculated spectrum with respect to band positions and relative intensities. Many of the modes have been excluded from Table 1 in this region. They generally comprise out-of-plane and in-plane C–C–C, C–H, N–H and C–C–N angle deformations. The Raman active modes are mostly very weak, involving many of the atoms in the molecule in unique movements, typically compressing or elongating parts of the molecule in one direction as well as rotations involving also larger parts of the molecule. However, some of the modes deserve attention, especially the four observed bands at around 721, 616, 463 and 218 cm^{-1}, which are interesting because they may have analytical applications. This is so because their intensities seem to be selectively enhanced by the green laser (Fig. 2 bottom right). Looking at the corresponding modes in the calculation (Table 1), it appears that they all involve displacements around the chromophoric azo group, suggesting strongly that the intensity enhancement is caused by the RR phenomenon related to electronic absorption in the hydrazo group.

To conclude, the calculated spectrum overall fits the experimental results quite well. The calculations suggest that the nature of the bands at around 1600–1500 cm^{-1} are rather complex but have been oversimplified in previous studies. In accordance with these previous studies, we also assign many of these vibra-

Table 1. Experimental Raman spectrum (cm^{-1}) compared to the calculated modes of the Sudan I in the hydrazo form

Mode no.	Experimental[a] cm^{-1}	Intensity	Calculated[b] cm^{-1}	Intensity $Å^2$/amu	Assignments[c]
87			3139	35	C–H stretch (ph)
86			3132	55	C–H stretch (naph)
85	3067	vw	3118	380	C–H stretch (ph)
84			3117	209	C–H stretch (naph)
83			3112	306	C–H stretch (naph)
82	3059	sh	3106	157	C–H stretch (ph) + N–H stretch
81			3105	747	N–H stretch
80			3097	110	C–H stretch (ph)
79	3039	vw	3096	133	C–H stretch (naph)
78			3091	17	C–H stretch (ph)
77			3087	90	C–H stretch (naph)
76			3079	64	C–H stretch (naph)
75	1616	sh	1621	60	C=O + C=C stretch (naph ring 2) + N–H bend
74	1600	sh	1606	101	C–H ip bend (naph) + C=C stretch (naph) + N–H bend + N=N/C–N stretch
73	1596	vs	1598	2378	C–H ip bend (ph) + C=C stretch (ph) + N–H bend + N=N/C–N stretch
72			1590	122	C1–N–H scis + C=C stretch (ph + naph) + C–H bend
71			1572	80	C1–N–H scis + C=O stretch + C=C stretch + C–H bend
70	1546	m	1545	164	C=C stretch (naph) + H–N=N bend + C=O stretch
69			1528	955	H–N=N bend + N=N stretch + N=C9 stretch + C=O stretch
68	1494	s	1488	723	C=C stretch (ph) + C–H ip bend (ph)
67	1481	sh	1475	104	C=C stretch (naph) + C=O stretch + N=H + C–H ip bend
65	1448	s	1444	181	C–H + N–H ip bend + asym C–C stretch (naph)
64	1410	sh	1397	337	C–N stretch (ph + naph) + N–H ip bend + C–H ip bend
63	1388	s	1391	750	C–N stretch (ph + naph) + C=O stretch + C–H ip bend
	1370	sh			
62	1340	m	1328	109	N=N + C=O stretch + C=C (ph) stretch/C–H ip bend (ph)
61	1333	sh	1321	273	C=C stretch (naph)/C–H ip bend (naph) + N–C9 stretch
60	1322	sh	1317	464	C=C–N bend (ph + naph) + N=N stretch + C=C stretch + ip N–H bend
59	1298	vw	1300	46	N=N + C=O + C=C stretch, ip N–H and C–H bend
58			1287	288	N=N stretch + N–H ip bend, N–H ip bend, C=O stretch
57	1257	m	1242	220	C9–C10–C12 stretch and bend + C–H ip. bend (naph)
56	1227	s	1228	1182	C–H + N–H ip bend + N–C1 stretch C=C stretch (naph)
55	1203	w	1205	70	C–H ip bend + C–N stretch + C=C stretch (naph)
54	1184	w/sh	1181	12	C–H + N–H ip bend + N–C1 stretch + C–C–C bend
53	1169	m	1161	403	C–H + N–H ip Bend N–C1 stretch + C–C–C bend
52	1151	w	1154	20	C–H ip bend and C–C–C bend
51	1140	sh.	1151	70	C–H + N–H ip bend and C–C bend
50	1118	Sh	1130	24	C–H ip bend and C–C–C bend (naph)
49	1095	w/m[d]	1093	60	ip C–C–C bend/stretch + C–H bend + C=N stretch

Table 1. (*continued*)

Mode no.	Experimental[a] cm^{-1}	Intensity	Calculated[b] cm^{-1}	Intensity $Å^2$/amu	Assignments[c]
48	1072	vw	1076	9	ip C–H bend + C–C–C bend + stretch
47	1038	vw	1035	38	C–H ip bend + asym breathing + C=C stretch (naph)
46	1018	vw	1018	14	asym breathing + C=C stretch (ph) + ip C–H bend (ph)
45	1001	m	988	167	triang breathing (ph) + N=N–C (naph) + N–H ip bend
43	984	m	980	202	N=N–C (naph) + H–N bend + breathing (ph) + (naph ring 3) breathing + C–C stretch (C9–C10)
34	846	vw	843	21	N–N–H bend + C–N=N (ph) bend + C–H ip bend
30	752	vw	750	6	C–H oop bend (ph)
28			744	20	C–N stretch (ph) + C=C bend (ph + naph) + C=C stretch (naph)
27	721[e]	vw/m[d]	718	59	breathing (naph) + C–C–N + N=N–C + C=C–C ip bend (ph)
	651	vw			
23	616[e]	vw/m[d]	616	14	C=C–C ip bend (ph) + C–C–N ip bend (ph + naph)
22	585	vw	583	57	C=C–C ip bend + ip N–N–C bend (ph + naph) + C=O ip bend
21	525	vw	540	4	C=C–C ip bend + ip N–N–C bend (ph + naph)
	501	vw			
16	463[e]	vw/m[d]	460	19	C=C–N ip bend + C=C–C ip bend + C–C=O ip bend
15			419	12	C=C–N ip bend + C=C–C ip bend (naph)
11	362	vw	361	22	N–C–C ip bend (ph + naph) out of phase
	310	vw			
7	218[e]	vw/m[d]	211	6	N–C–C ip bend (ph + naph) in phase
6	159	vw	179	3	C–C–H, C=C–C, N=N–C oop bend

Assignments (approximate descriptions of the modes) have been obtained from the calculated gas phase results [Gaussian/DFT/B3LYP/6-311+G(d,p)] observing the modes on a computer screen. Certain modes have been omitted to make the table shorter.
[a] The given measured wavenumbers were obtained on the Bruker FT-instrument.
[b] The calculated wavenumbers have been corrected with a factor of 0.976 according to Fairchild *et al.*[19]
[c] Stretch, stretching; bend, bending; ip, in-plane; oop, out-of-plane; asym, asymmetric; sym, symmetric; scis, scissoring; triang, triangular; ph: phenyl ring; naph, naphthyl ring.
[d] These bands were significantly enhanced when using the green laser.
[e] Analytically interesting bands, see text.

tions to modes with pronounced C–C stretching in phenyl and naphthalene rings.[11,22,23] However, our calculations show that other modes such as movements within the hydrazo group also contribute significantly. Our calculations also indicate that the hydrazo group is involved in most of the vibrations through N–H and C–N=N bendings and C–N stretchings. The hydrazo group also is the chromophore in the molecule, and therefore these features make the Sudan I molecule very suitable for RR spectroscopic investigations.

The intensities of the bands below 900 cm^{-1} seem to be quite sensitive to the laser wavelength and the sample environment. A similar effect was reported in Refs [9 and 10] concerning the spectra of the related azo dyes Sudan II and Sudan IV. Sudan II has the same structure as Sudan I, but with two methyl groups substituted on the phenyl ring in ortho and para positions. Sudan IV also has a methyl group on the phenyl ring in the ortho position, but has a further azo-toluene unit on the first phenyl ring in the para posistion. SERS spectra of Sudan II on various nanowire areas with IR excitation (1064 nm) have shown very similar trends, although they depend somewhat on the type of the metal substrate used.[9] Similarly, for Sudan IV the SERS spectrum below 1000 cm^{-1} has been recorded with IR excitation (1064 nm), showing several new features not seen in the regular Raman spectrum.[10]

Similarities between Azo Dyes

The Raman spectrum of Sudan I has striking similarities with the Raman spectra of other similar azo dyes. Because of their low toxicity, many sulfonated azo dyes are widely used in the food industry. The use of Raman spectroscopy for the detection of toxic azo dyes therefore demands a specific knowledge about other similar azo dyes. A typical example is Orange II, which is very similar to Sudan I, the only difference being a single SO_3Na group substituted in para position to the C–N group in the phenyl ring. The spectrum in the region from 1600 to

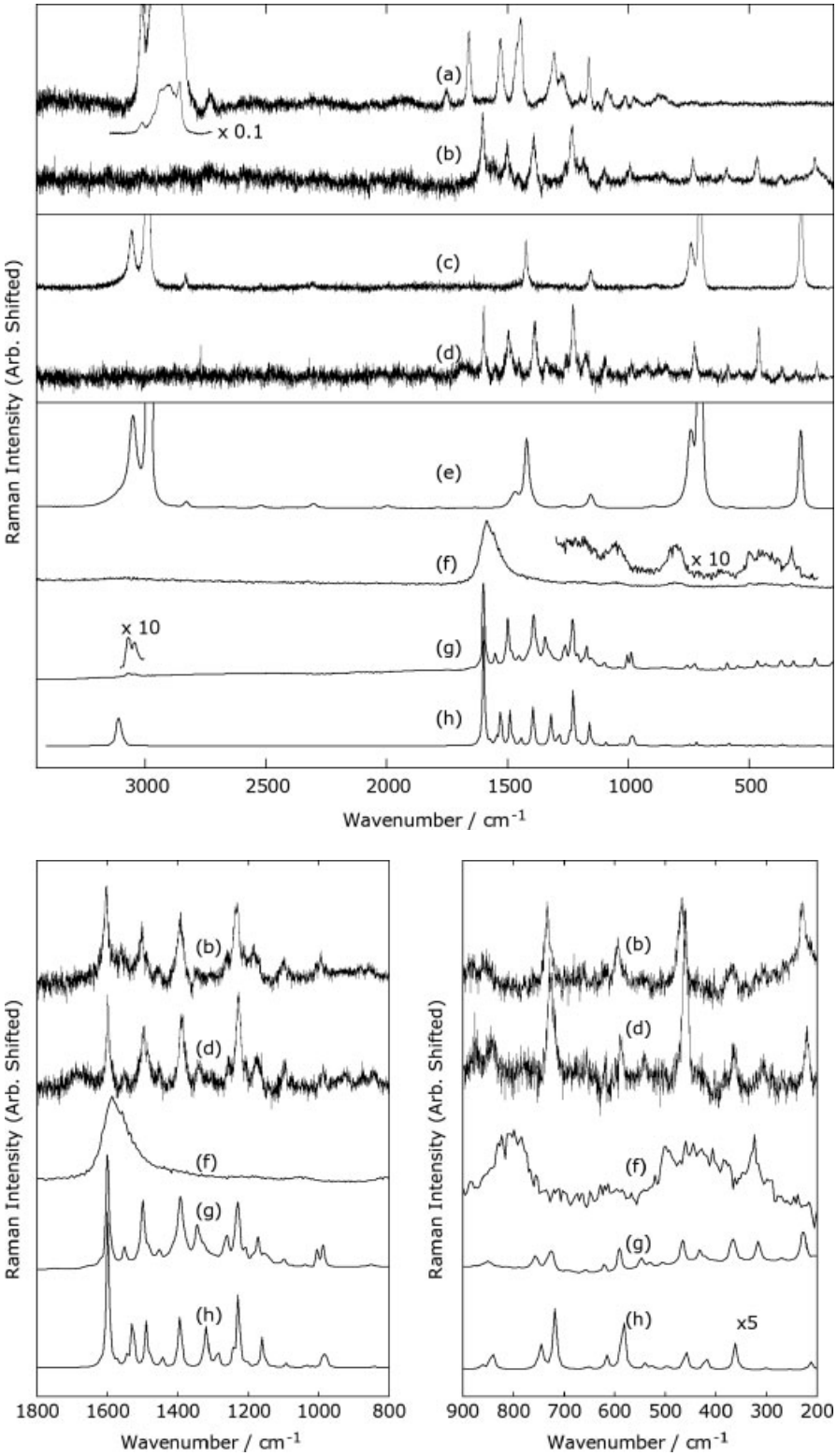

Figure 2. Raman spectra of (a) pure olive oil (excitation: green laser, 532 nm), (b) Sudan I in olive oil (nearly saturated. Excitation: green laser, 532 nm), (c) pure CH_2Cl_2 (excitation: green laser, 532 nm), (d) Sudan I in CH_2Cl_2 (excitation: green laser, 532 nm), (e) pure CH_2Cl_2 (excitation: UV laser, 244 nm), (f) Sudan I in CH_2Cl_2 (nearly satureted. Excitation: UV laser, 244 nm), (g) Sudan I powder (excitation: infrared laser, 1064 nm) and (h) calculated Raman spectrum, wavenumber corrected with a factor of 0.976. Top: Full spectra. Bottom left: Zoom of the region 1800–900 cm^{-1}. Bottom right: Zoom of the region 900–200 cm^{-1}. Note: In the top graph, the spectrum of the C–H stretching region of (a) is also shown, decreased by a factor of 0.1, and for spectra (f) and (g) selected parts are also shown, magnified by a factor of 10. The spectra have also been arbitrarily scaled and shifted. The band at 2331 cm^{-1} in (c) and (e) is due to N_2 gas.

Journal of RAMAN SPECTROSCOPY

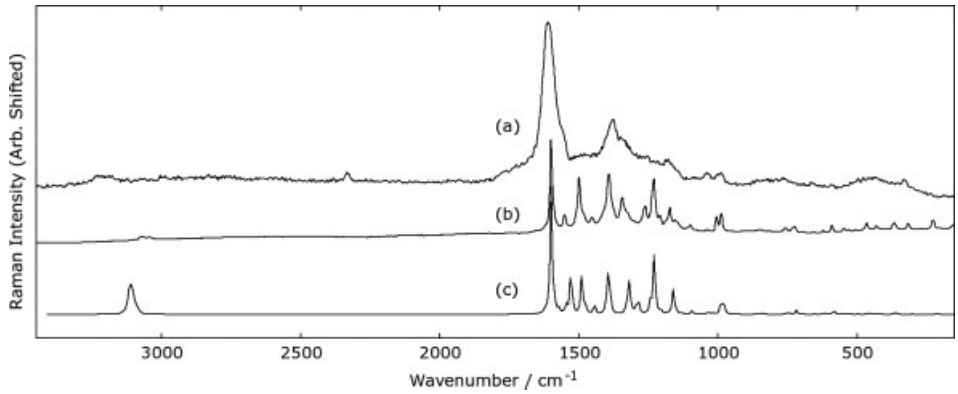

Figure 3. Raman spectra of solid Sudan I obtained with (a) 244 nm UV light and (b) 1064 nm IR light. Useful spectra could not be obtained with green or blue light. The calculated spectrum is shown as (c). The band at 2331 cm^{-1} in (a) is due to N_2 gas.

1300 cm^{-1} shows almost identical features. Below this region, the spectra look very similar, but larger deviations in the wavenumber shift values occur.[23] Also, the azo dye Amaranth (Azorubin S or tri-sodium (4*E*)-3-oxo-4-[(4-sulfonato-1-naphthyl)hydrazono]-naphthalene-2,7-di-sulfonate, CAS Reg. No. 915-67-3), previously much used in foodstuffs, can be described as a triple sulfonated double naphthyl analog of Sudan I. Although the spectra look very similar to that of Sudan I in the region 1600–1100 cm^{-1}, the values of the Raman shifts deviate sufficiently to distinguish them.[22]

The structure of the sulfonated yellow azo dye Tartrazine (1*H*-pyrazole-3-carboxylic acid, 4,5-dihydro-5-oxo-1(4-sulfophenyl)-4-[(4-sulfophenyl)azo] tri-sodium salt, CAS Reg. No. 1934-21-0) differs more from the structure[21] of Sudan I. Although the spectrum in the range 1600–1480 cm^{-1} shows very similar features, many wavenumber shift values deviate considerably. At lower wavenumbers, the spectra deviate more from each other, and below 1000 cm^{-1} the Raman active bands are entirely unique.

Natural abundant cartenoids give colors to biological materials such as plants, and are therefore present in most foodstuffs. Especially capsanthin [(all-*E*,3*R*,3′*S*,5′*R*)-3,3′-dihydroxy-β,κ-caroten-6′-one, CAS Reg. No. 465-42-9] and capsorubin [(all-*E*,3*S*,3′*S*,5*R*,5′*R*)-3,3′-dihydroxy-κ,κ-carotene-6,6′-dione, CAS Reg. No. 470-38-2], found in chili and paprika, makes it difficult to detect Sudan I in samples because they exhibit Raman and absorption maxima at similar wavenumbers as in Sudan I.[2,13] The Raman spectra of capsanthin and capsorubin were investigated by DFT calculations as well as experimentally by Requena *et al*.[24] Even though the structures are very different, many Raman bands for capsanthin and capsorubin are found at more or less the same positions[24] in the region from 1600 to 1100 cm^{-1}. The best way to distinguish these molecules by Raman spectroscopy is to take advantage of some very intense bands in the spectra of capsanthin and capsorubin at around 1100–900 cm^{-1}, where the spectrum of Sudan I only shows weaker features as well as the considerable contribution to the spectra from C–H stretching in the spectra of the cartenoids.

Resonance Raman Effects

Shadi *et al*. at an ICORS conference reported resonance enhancement of the peaks in Sudan I at 1234 and 1598 cm^{-1} when using a 632.8 nm laser.[8] This feature is supported by our calculations, which just show contribution to those bands from C–N bending and stretching modes in the hydrazo chromophore group. The RR effects in Sudan I spectra have systematically been investigated by Munro *et al*.[11] in the range 1180–1618 cm^{-1}. Using different laser wavelengths from 501 to 613 nm, they observed that a 501 nm green laser line gave the strongest RR effect in this region of the spectra.[11] According to their calculations, which were based on the low level semiempirical PM3 method, the vibrations in this part of the spectrum were mostly due to isolated C–C vibration modes, whereas our calculations show rather significant contributions from C–C–N bendings as well as C–N and N═N stretchings in this region. Additional peaks below 1100 cm^{-1} were also amplified because of RR effects when using a 613 nm laser.

The spectrum of Sudan I in olive oil measured with the 532 nm laser clearly showed an enhancement of several orders of magnitude for the intensity of the bands at 721, 616, 463 and 218 cm^{-1}. In Fig. 4(f)–(h), three diagrams of the corresponding calculated modes can be seen (modes 23, 16 and 7), and it is obvious that they all involve extended bending of the C–N–N–C skeleton. Though overtones and progressions could not be found (perhaps due to overlaps with more intense bands), it still is an indication of a RR effect arising from these vibrations. The resonance at these wavenumbers has a potential use as a means to distinguish Sudan I from other azo dyes because this RR pattern is likely to be unique. A procedure involving different laser wavelengths could supply a unique fingerprint for Sudan I due to its specific resonance enhancement at lower wavenumbers, as used widely in the pharmaceutical industry.[25] Also, we believe that this, in combination with the results of Cheung *et al*.,[12] indicates that SERRS with different excitation wavelengths in the fingerprint region, can indeed provide a useful technique for the detection of Sudan I in foodstuffs.

Conclusion

Raman spectra of the red dye Sudan I were recorded using infrared (1062 nm), green (532 nm) and UV (244 nm) laser light. The spectra were interpreted by comparison with *ab initio* DFT (RB3LYP) calculated spectra, based on 6-311+G(d,p) Gaussian orbital basis sets in an isolated molecule approach. The vibrations in the region 1600–1000 cm^{-1} were found to comprise various mixed modes including in-plane stretching of C–C bonds. Especially, the large contributions from N═N core stretching and C–N–N bond bending at higher wavenumbers have not been appreciated previously. Below about 900 cm^{-1}, many out-of-plane bending modes were dominant. Low-intensity bands at 721, 616, 463 and 218 cm^{-1} were selectively enhanced by the RR effect, when using

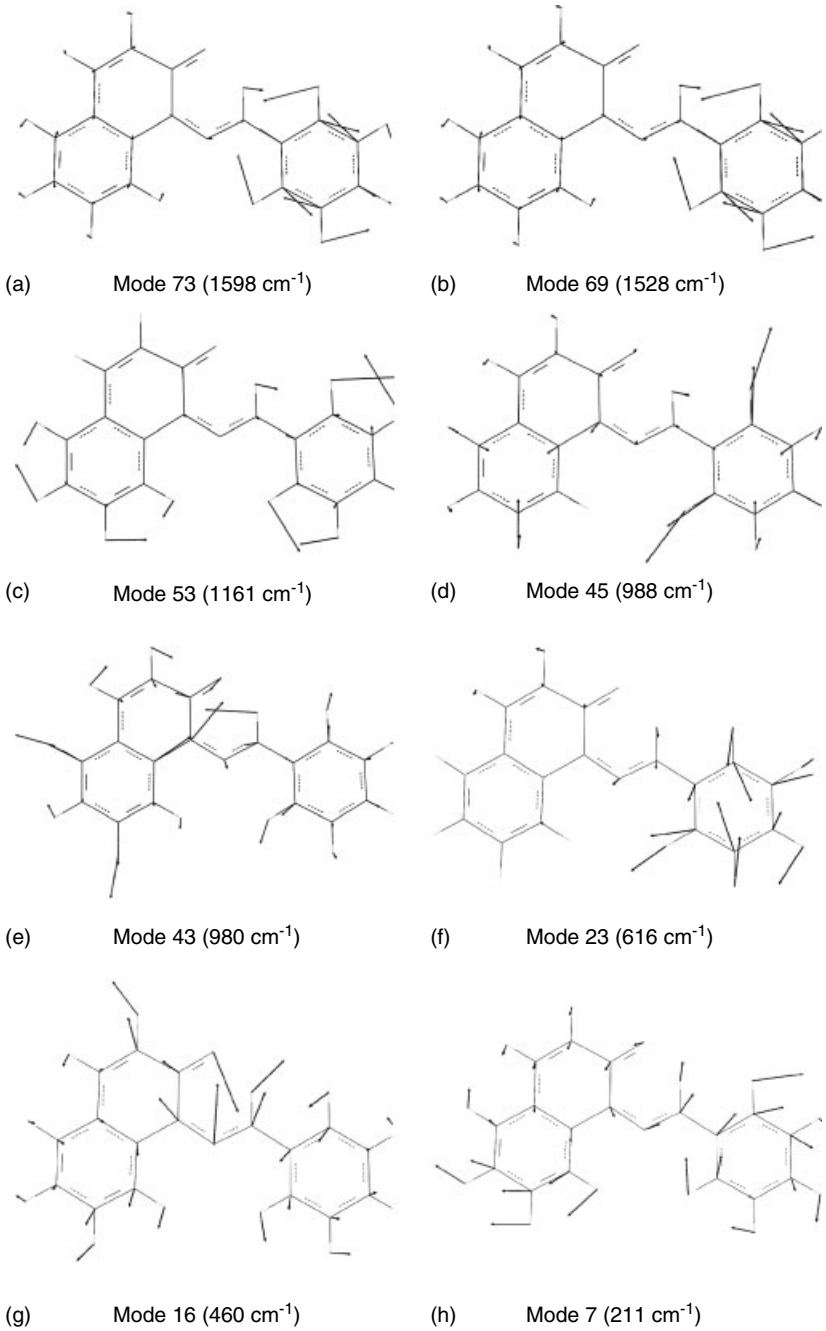

Figure 4. Approximate diagrams of selected vibrations in the hydrazo form of Sudan I. The presented wavenumbers have been corrected with an empirical scaling factor of 0.976[19].

the 532 nm excitation line, relative to those obtained with 1064 or the 244 nm excitation. The spectrum of Sudan I was found to deviate from those of other similar azo dyes, even in the intensive range (1600–1000 cm^{-1}). The spectra of abundant natural food pigments, such as capsanthin and capsorubin showing similar Raman active bands in the same wavenumber range, can be distinguished from those of Sudan I by the spectral differences below 1100 cm^{-1}. The use of differences in the resonance enhancement of various bands (marked with stars in Table 1) with the applied lasers opens up a new sensitive method to detect Sudan I in food based on Raman spectroscopy. Our *ab initio* DFT calculations have indicated that several vibrations in the whole investigated wavenumber range involve bending and stretching modes – at and around the C–N═N–C chromophore – making the molecule obvious for further investigations with SERRS and/or SERS.

Acknowledgements

We would like to thank Lykke Ryelund from University of Copenhagen for help in obtaining the FT-Raman spectra. Udo Jensen at Fødevareregion Øst, Fødevarestyrelsen, Ringsted DK, is thanked for providing the sample of Sudan I. The Danish Agency for Science Technology and Innovation provided a grant (No. 09-065038/FTP) for CL and the UV instrumentation.

References

[1] V. Cornet, Y. Govaert, G. Moens, J. V. Loco, J. J. Degroodt, *J. Agric. Food Chem.* **2006**, *54*, 539.
[2] H. Buchardt, *Dan. Kemi* **2007**, *88*, 28.
[3] P. Møller, H. Wallin, *Mutat. Res. Rev. Mutat. Res.* **2000**, *462*, 13.
[4] M. Stiborova, V. Martinek, H. Rydlova, P. Hodek, E. Frei, *Cancer Res.* **2002**, *62*, 5678.
[5] F. Tateo, M. J. Bononi, *J. Agric. Food Chem.* **2004**, *52*, 655.
[6] F. Puoci, C. Garreffa, F. Iemma, R. Muzzalupo, U. G. Spizzirri, N. Picci, *Food Chem.* **2005**, *93*, 349.
[7] M. Mazzetti, R. Fascioli, I. Mazzoncini, G. Spinelli, I. Morelli, A. Bertoli, *Food Addit. Contam.* **2004**, *21*, 935.
[8] I. T. Shadi, B. Z. Chowdhry, S. A. Leharne, R. Withnall, *ICORS20, 20th International conference on Raman Spectroscopy*, vol. 20 Wiley: Yokohama, Japan, **2006**, pp. 247.
[9] L. S. Zhang, P. X. Zhang, Y. Fang, *J. Colloid Interface Sci.* **2007**, *311*, 502.
[10] X. F. Zhou, Y. Fang, P. X. Zhang, *Spectrochim. Acta, Part A* **2007**, *67*, 122.
[11] C. H. Munro, W. E. Smith, D. R. Armstrong, P. C. White, *J. Phys. Chem.* **1995**, *99*, 879.
[12] W. Cheung, I. T. Shadi, Y. Xu, R. Goodacre, *J. Phys. Chem. C* **2010**, *114*, 7285.
[13] M. I. Minguez-Mosquera, M. Jaren-Galan, J. Garrido-Fernandez, *J. Agric. Food Chem.* **1992**, *40*, 2384.
[14] R. W. Berg, A. Riisager, R. Fehrmann, *J. Phys. Chem. A* **2008**, *112*, 8585.
[15] R. W. Berg, M. Deetlefs, K. Seddon, I. Shim, K. Thompson, *J. Phys. Chem. B* **2005**, *119*, 19018.
[16] M. H. Brooker, R. W. Berg, J. H. von Barner, N. J. Bjerrum, *Inorg. Chem.* **2000**, *39*, 4725.
[17] R. W. Berg, I. M. Ferré, S. C. Schäffer, *J. Vib. Spectrosc.* **2006**, *42*, 346.
[18] M. J. Frisch, H. B. Schlegel, G. E. Scuseria, M. A. Robb, J. R. Cheeseman, J. A. Montgomery Jr, T. Vreven, K. N. Kudin, J. C. Burant, J. M. Millam, S. S. Iyengar, J. Tomasi, V. Barone, B. Mennucci, M. Cossi, G. Scalmani, N. Rega, G. A. Petersson, H. Nakatsuji, M. Hada, M. Ehara, K. Toyota, R. Fukuda, J. Hasegawa, M. Ishida, T. Nakajima, Y. Honda, O. Kitao, H. Nakai, M. Klene, X. Li, J. E. Knox, H. P. Hratchian, J. B. Cross, C. Adamo, J. Jaramillo, R. Gomperts, R. E. Stratmann, O. Yazyev, A. J. Austin, R. Cammi, C. Pomelli, J. W. Ochterski, P. Y. Ayala, K. Morokuma, G. A. Voth, P. Salvador, J. J. Dannenberg, V. G. Zakrzewski, S. Dapprich, A. D. Daniels, M. C. Strain, O. Farkas, D. K. Malick, A. D. Rabuck, K. Raghavachari, J. B. Foresman, J. V. Ortiz, Q. Cui, A. G. Baboul, S. Clifford, J. Cioslowski, B. B. Stefanov, G. Liu, A. Liashenko, P. Piskorz, I. Komaromi, R. L. Martin, D. J. Fox, T. Keith, M. A. Al-Laham, C. Y. Peng, A. Nanayakkara, M. Challacombe, P. M. W. Gill, B. Johnson, W. Chen, M. W. Wong, C. Gonzalez, J. A. Pople, *Gaussian 03 W, Revision E.01*, Gaussian, Inc.: PA, USA, **2006**.
[19] S. Z. Fairchild, C. F. Bradshaw, W. S. Su, S. K. Guharay, *Appl. Spectrosc.* **2009**, *63*, 733.
[20] J. E. Bertie, K. H. Michaelian, *J. Chem. Phys.* **1998**, *109*, 6764.
[21] N. Peica, I. Pavel, S. C. Pinzaru, V. K. Rastogi, W. Kiefer, *J. Raman Spectrosc.* **2005**, *36*, 657.
[22] M. Snehalatha, C. Ravikumar, N. Sekar, V. S. Jayakumar, I. H. Joe, *J. Raman Spectrosc.* **2008**, *39*, 928.
[23] L. C. Abbott, S. N. Batchelor, J. Oakes, B. Gilbert, A. C. Whitwood, J. R. L. Smith, J. N. Moore, *J. Phys. Chem. A* **2005**, *109*, 2894.
[24] A. Requena, J. P. Ceron-Carrasco, A. Bastida, J. Zuniga, B. Miguel, *J. Phys. Chem. A* **2008**, *112*, 4815.
[25] J. A. Zeitler, D. A. Newnham, P. F. Thaday, T. L. Threlfall, R. W. Lancaster, R. W. Berg, C. J. Strachan, M. Pepper, K. C. Gordon, T. Rades, *J. Pharm. Sci.* **2006**, *95*, 2486.